

# BARELY VISIBLE IMPACT DAMAGE DETECTION IN SANDWICH STRUCTURES USING NON-UNIFORM STRAIN ALONG OPTICAL FIBER SENSORS

**Shu Minakuchi\*, Yoji Okabe\*, Nobuo Takeda\***

\*The University of Tokyo

*Keywords:* sandwich structure, impact damage, optical fiber, PPP-BOTDA, non-uniform strain

## Abstract

Impact damage detection system for sandwich structures was developed by using a specific response of pre-pump pulse Brillouin optical time domain analysis (PPP-BOTDA) sensing system to non-uniform strain distribution along an optical fiber. The innovative PPP-BOTDA sensing system employs stimulated Brillouin scattering in the optical fiber and realizes distributed strain measurement with spatial resolution of 10 cm, sampling interval of 5 cm and sensing range of more than 1 km. First, it was revealed that strain gradient broadens a width of a Brillouin gain spectrum, which is a respondency of the PPP-BOTDA. Then the specific response of the PPP-BOTDA was employed to detect non-uniform strain distribution along a dent of the facesheet in a damaged area. As the damage became larger, the width of the Brillouin gain spectra became broader. Consequently, location and size of barely visible damage could be estimated. The developed system can be used in a first inspection of large sandwich structures in aerospace applications.

## 1 Introduction

Composite sandwich structures are attracting much attention as a solution to maximize realization of potentials of advanced composite materials [1-3]. The composite sandwich structures are integral constructions consisting of two composite facesheets and a lightweight core. The facesheets primarily resist the in-plane and lateral (bending) loads, and the core keeps the distance between two facesheets and carry transverse forces. Since the composite sandwich structures have extremely high specific stiffness and inherent multifunctionality, they are expected to be applied to primary structures in aerospace applications [2, 4]. However, since the composite facesheet is very thin and the lightweight

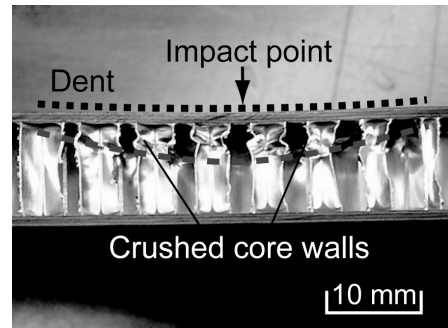


Fig. 1. Cross-sectional view of impact damage

core is weak, they can be easily damaged when impact or indentation load is applied [5, 6]. The core under loading point crushes and a dent of the facesheet remains, as presented in Fig. 1. The dent significantly deteriorates the stiffness and strength of sandwich structures, even when it is small and barely visible. The perturbed geometry of the facesheet and degraded mechanical property of the damaged core alters the stress field in the structures, and, as a result, damages in the facesheet and the core initiate under considerably low loading condition [7, 8]. The authors have developed a new 'segment-wise model' to simulate indentation response of honeycomb sandwich structures by taking into account periodical geometry and complicated crushing/stretching behavior of honeycomb core [9]. It was revealed that the dent of the facesheet is introduced by severely damaged core near the loading point and the dent generates significantly high residual stress field in an undamaged part of the core, which could be a source of further damage progress. It was also confirmed that relatively high non-uniform strain is induced along the convex and concave part of the facesheet (Fig. 2). Residual strain of more than 1000  $\mu\epsilon$  remains on the facesheet even in the case of invisible damage (residual dent depth: < 2.5 mm) [10].

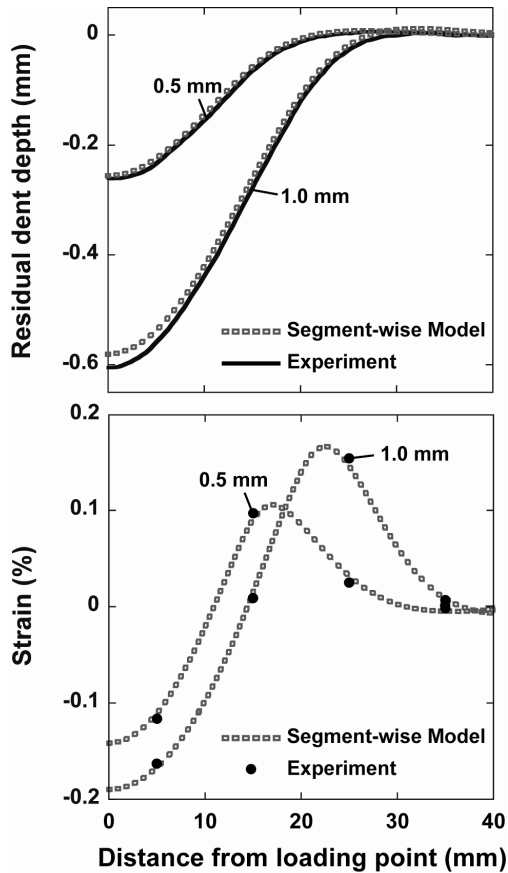


Fig. 2. Profiles of residual dents of facesheet and non-uniform strain distribution along the dent in aluminum honeycomb sandwich beams [10]

(The values in the graph denote applied maximum indentation depth)

In this study, impact damage is detected by measuring the residual strain along the dent of the facesheet using a specific response of PPP-BOTDA.

The developed system realizes barely visible impact damage monitoring of large aerospace structures with a very limited number of the optical fiber. First, the specific response of the PPP-BOTDA is revealed by comparing Brillouin gain spectra obtained in a tensile test and a three-point bending test. Then a validity of the proposed impact damage detection system is confirmed through damage detection in a honeycomb sandwich panel, where a single optical fiber is embedded in the adhesive layer at even intervals of 5 cm.

## 2 Specific response of PPP-BOTDA to non-uniform strain

A schematic of the PPP-BOTDA sensing system (Neubrescope, Neubreex Co., Ltd) is illustrated in Fig. 3. The PPP-BOTDA sensing system employs a stimulated Brillouin scattering (SBS) technique [11]. Two laser beams, a pump pulse, which has unique wave profile, and a continuous wave (CW) probe light, are injected into an optical fiber from both its ends. The interaction of these two laser beams excites acoustic waves, due to their different frequencies. The pump pulse is backscattered by the phonons, and part of its energy is transferred to the CW. The power gain of the CW, which is called the Brillouin gain spectrum (BGS), as a function of frequency difference between the two laser beams, is measured at the output end of the probe light while the frequency of the probe light is scanned. The value of the strain can be estimated by measuring the peak frequency of Brillouin gain spectrum (Brillouin frequency), while its position along the fiber is calculated from the light round-trip time. This measuring system realizes spatial

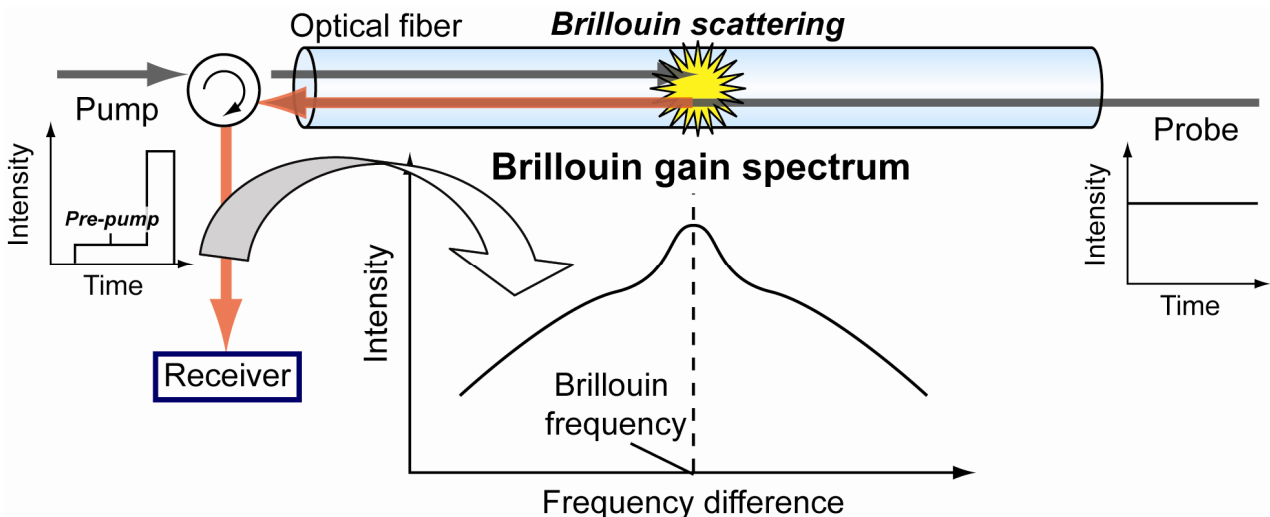


Fig. 3. Schematic of PPP-BOTDA sensing system

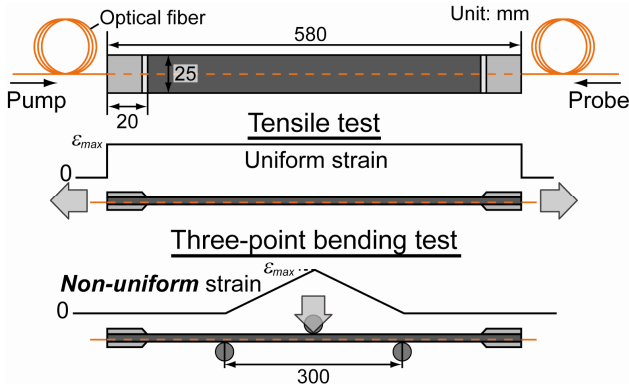
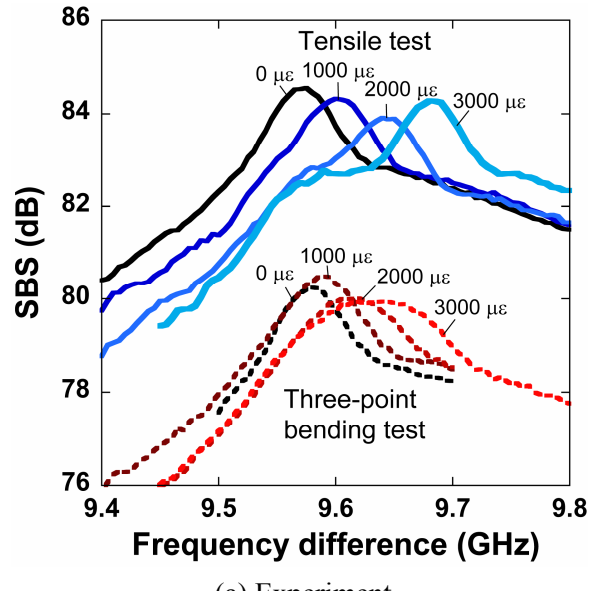


Fig. 4. Specimen for tensile test and three-point bending test

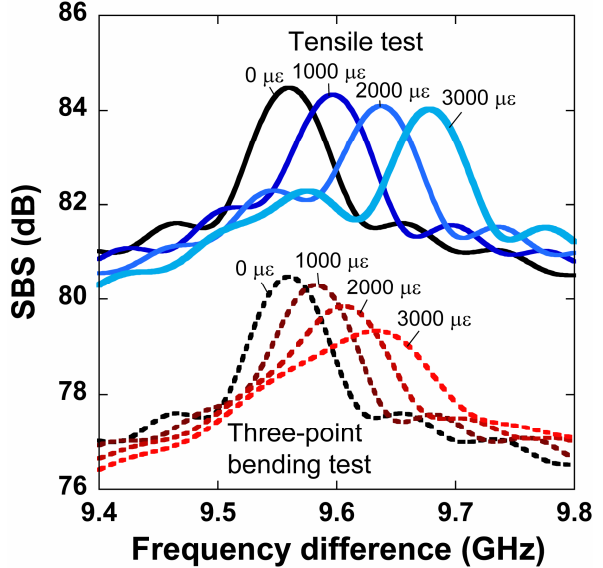
resolution of 10 cm, sampling interval of 5 cm, and sensing range of more than 1 km with  $\pm 0.0025\%$  strain measurement accuracy [12]. The PPP-BOTDA sensing system have been successfully utilized for distributed strain measurement of large structures [13], where strain gradient is considerably moderate and the strain distribution is almost uniform within the spatial resolution of 10 cm. Meanwhile, the response of the PPP-BOTDA sensing system to non-uniform strain distribution within the spatial resolution is not sufficiently understood.

In order to reveal the response of the PPP-BOTDA, a tensile test and a three-point bending test were conducted using a single specimen. A schematic of the specimen is illustrated in Fig. 4. The optical fiber was embedded in the interface between the 6th and 7th ply of a carbon fiber reinforced plastic (CFRP) laminate (T700S/2500, Toray Industry, Inc., [0<sub>8</sub>]). This experiment was intended to clarify an effect of strain gradient on the shape of the BGS by comparing the spectra obtained in the tensile test and the three-point bending test, where the strain distribution is uniform and non-uniform, respectively. In both tests, the spectra were measured when the strain at the center of the specimen  $\varepsilon_{max}$  was 1000  $\mu\epsilon$ , 2000  $\mu\epsilon$ , and 3000  $\mu\epsilon$ . Obtained spectra are presented in Fig. 5 (a). For clear appearance, the spectra in the bending test are shown after purposely decreasing their intensity. In the tensile test, the spectrum retained its shape while the Brillouin frequency shifted to the higher frequency side, corresponding to the strain increase. In the bending test, on the other hand, the shape of the spectra became gentle as the strain increased and the strain gradient became steep.

The effect of the non-uniform strain was also evaluated through simulation of the spectra. The theory for the phenomena included in the PPP-



(a) Experiment



(b) Analysis  
Fig. 5. BGS obtained in tensile test and three-point bending test

BOTDA sensing system has been recently developed by solving coupled wave equations by a perturbation method [12] and thus the response of PPP-BOTDA to arbitrary strain profiles can be numerically simulated. Calculated spectra are presented in Fig. 5 (b). As in the experiments, the steeper the strain gradient became, the more spectrum width broadened, while the spectrum kept its shape in the tensile test.

The effect of the strain profile on the shape of the BGS can be interpreted as below. When the uniform strain is applied to the optical fiber, the Brillouin frequency is also uniform, and thus the

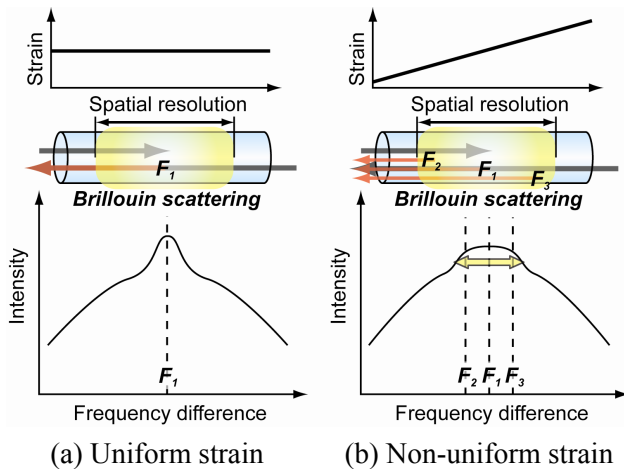


Fig. 6. Response of PPP-BOTDA to various strain profiles

BGS has only one sharp narrow peak (Fig. 6 (a)). When the non-uniform strain is introduced, on the other hand, the Brillouin frequency also becomes non-uniform, since the Brillouin frequency at each point on the optical fiber is determined by the strain at the point. As a result, the BGS consisting of the entire Brillouin scattering along the spatial resolution becomes broad, as illustrated in Fig. 6. Moreover, the width of the BGS changes corresponding to the non-uniformity of the strain distribution.

As explained above, the PPP-BOTDA sensing system not only realizes distributed strain measurement with spatial resolution of 10 cm, but also responds to the non-uniform strain within the spatial resolution. In the following sessions, new impact damage detection system for large sandwich structures using the specific response of the PPP-BOTDA is proposed and validated through an indentation damage detection test.

### 3 Impact damage detection system

A schematic of the proposed system is illustrated in Fig. 7. The optical fibers are embedded

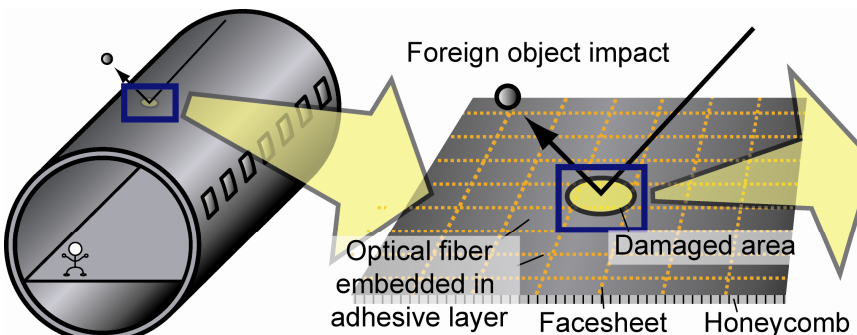


Fig. 7. Schematic of impact damage detection system for sandwich structures

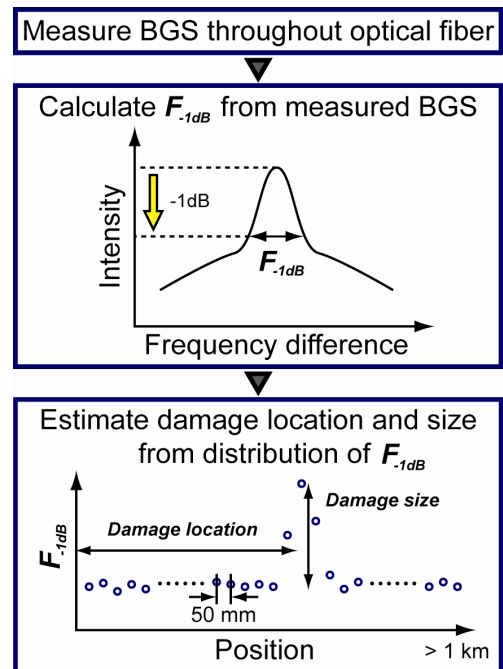


Fig. 8. Damage detection procedure using distribution of BGS width

in the adhesive layer between the facesheet and the core in a reticular pattern [3, 14]. Since the PPP-BOTDA has very long sensing range ( $> 1$  km), a limited number of the optical fibers are sufficient to cover the whole structure. When the impact damage is introduced, the residual dent of the facesheet induces tensile and compressive strain along the optical fiber at the concave and convex part. Consequently, the non-uniform strain broadens the width of the BGS obtained from the damaged area. Moreover, the width of the BGS broadens corresponding to impact damage size, since larger impact damage generates higher and wider non-uniform strain distribution along the residual dent of the facesheet (Fig. 2).

Damage detection procedure is specifically presented in Fig. 8. First, the Brillouin gain spectra are measured throughout the optical fiber embedded

in the whole structure or the area where the impact damage is suspected to be induced. Secondly, the width of each spectrum is calculated. Now, a full width at -1 dB from maximum  $F_{-1dB}$  (illustrated in Fig. 8) is selected as a representative value for the width of the BGS. When the impact damage is introduced, only the damaged area has unusually large value of  $F_{-1dB}$ , depending on extent of damage. Hence, damage location and size can be roughly estimated from the distribution of  $F_{-1dB}$  along the optical fiber. This proposed system must be useful in first inspection of impact damage in large sandwich structures. In the next section, the validity of the proposed system is confirmed by detecting barely visible damage in a honeycomb sandwich panel.

#### 4 Damage detection test

##### 4.1 Materials and methods

A schematic of the specimen is illustrated in Fig. 9. The sandwich panel consisted of CFRP facesheets (T700S/2500, Toray Industry, Inc., [0/90]<sub>3S</sub>, thickness of 1.5 mm), aluminum honeycomb core (AL 1/4-5052-001, Showa Aircraft Industry Co.) and thermoplastic adhesive films (AF-163-2K, 3M Co.). A single optical fiber was embedded between the preliminary molded upper facesheet and the adhesive layer. The upper facesheet was manufactured a little larger than the core and the lower facesheet for handling of the optical fiber. The experimental set-up is shown in Fig. 10. A hemispherical steel indenter, whose diameter was 12.7 mm, was attached to a material

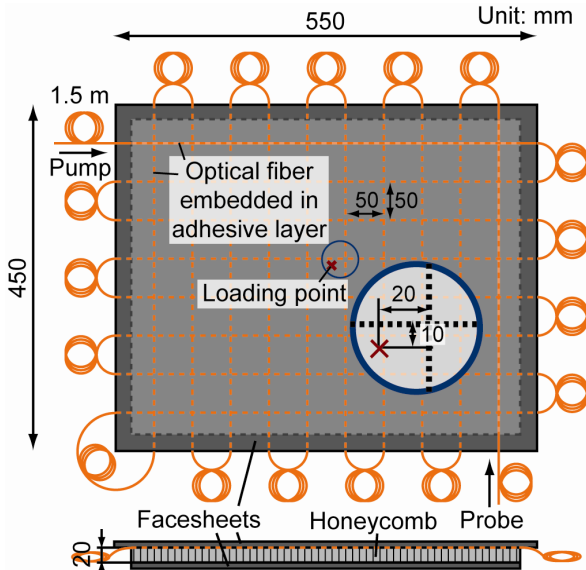


Fig. 9. Schematic of specimen for indentation damage detection test

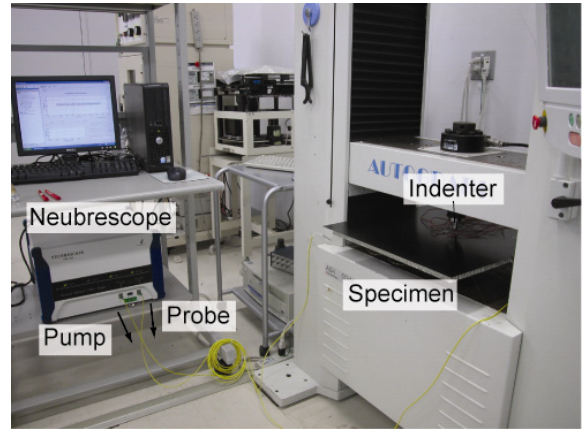


Fig. 10. Experimental set-up for indentation loading and BGS measurement

testing system (AG-50kNI, Shimazu Co.) and a quasi static point load was applied to near the center of the specimen in order to introduce simulated low velocity impact damage. After a predetermined maximum indentation displacement was reached, the crosshead reversely moved up. The tests of five kinds of the maximum displacement 1, 2, 3, 4, and 6.5 mm were conducted. After each test, the Brillouin gain spectra were measured throughout the specimen using the PPP-BOTDA sensing system (Neubrescope) connected to both ends of the optical fiber. By comparing the width of the spectra obtained in each test, the response of the proposed damage detection system depending on the damage size was investigated in detail. Additionally, damaged area was checked and recorded after each test by visual inspection and by using electric-resistance strain gages bonded at some points on the surface of the upper facesheet.

##### 4.2 Results

The load-displacement curves measured in all the tests are shown in Fig. 11. As the maximum indentation displacement increased, the residual dent

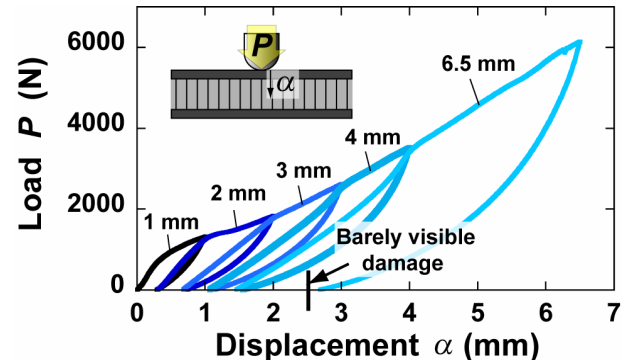


Fig. 11. Load-displacement curves obtained in indentation test

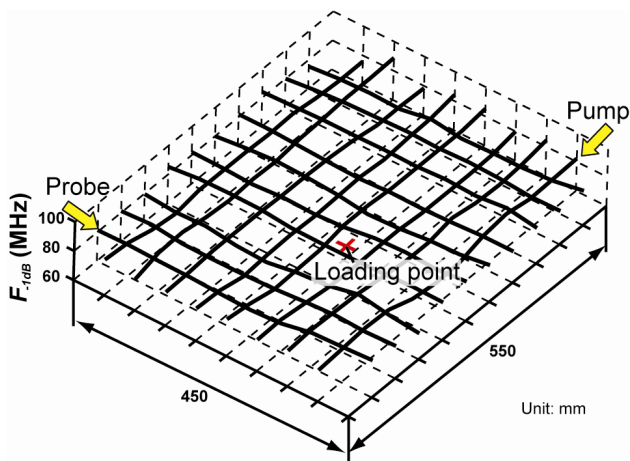


Fig. 12. Distribution of  $F_{1dB}$  in whole specimen before damage initiation

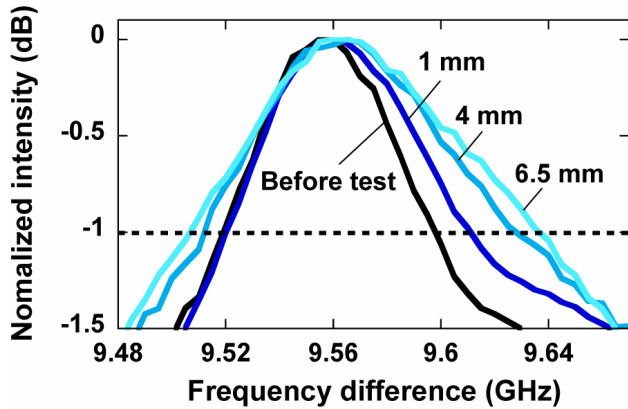


Fig. 13. Differences of BGS after each test measured at nearest measure point to loading point

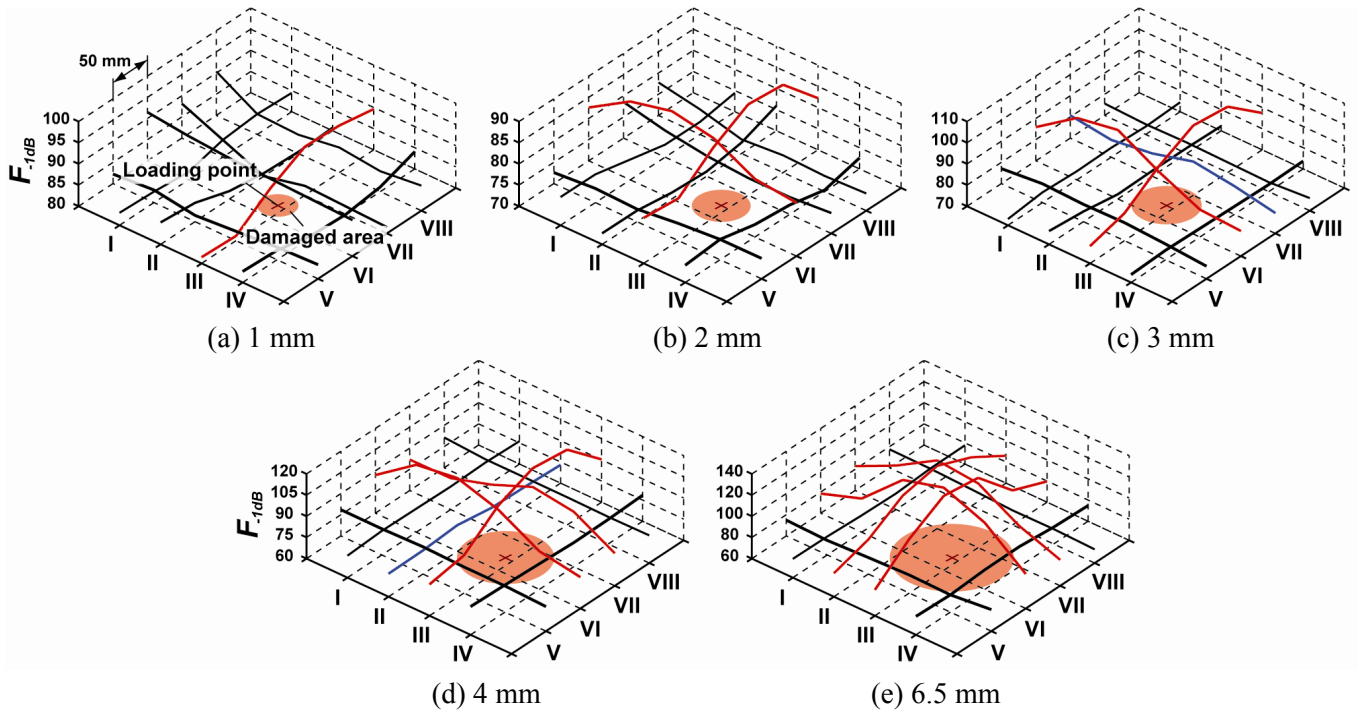


Fig. 14. Distribution of  $F_{1dB}$  at the center of specimen after each test

became deeper. Finally, a residual dent depth of 2.5 mm, which corresponds to the depth of barely visible impact damage (BVID), remained on the upper facesheet after the test of the maximum displacement 6.5 mm. Obtained distribution of  $F_{1dB}$  in the whole specimen before the test is presented in Fig. 12. Even though there were small fluctuations, the Brillouin gain spectra had almost uniform value of  $F_{1dB}$  of 80 MHz. However, after the damage was initiated, the non-uniform strain was generated along the dent of the facesheet and thus BGS started to broaden from the vicinity of the loading point. The spectra obtained at the nearest measure point to the loading point are presented in Fig. 13. The intensity of each spectrum was normalized by the intensity of the highest component. As the damage became larger, the width of the BGS gradually increased and finally became more than half time that before the test. The distributions of  $F_{1dB}$  after each test are presented in Fig. 14. Only the vicinity of the loading point is shown, since the other area did not mark significant changes in the width of the BGS. After the test of maximum indentation displacement of 1 mm (residual dent depth: 0.3 mm), only a line III of the optical fiber, which is the nearest to the loading point, responded and  $F_{1dB}$  increased near the damaged area due to the non-uniform strain along the dent of the facesheet. As the damage became large, both of a number of the responding lines and value of  $F_{1dB}$  near the damaged area increased. After the test of maximum indentation displacement of 3

mm (residual dent depth: 1.1 mm), two lines, i.e. III and VI, reacted significantly and one line of VII responded slightly. It is interesting to note that VI and VII were 20 and 30 mm away from the loading point, respectively. Even though a difference between the values of the distance from each line to the loading point was only 10 mm, the responses of both lines differed vastly, confirming quite high sensitivity and resolution of the proposed damage detection system. After the test of maximum indentation displacement of 6.5 mm (residual dent depth: 2.5 mm), all the four lines surrounding the loading point, i.e. II, III, VI, and VII, pronouncedly responded.

It was clearly demonstrated that the proposed damage detection system using the width of the BGS can detect an occurrence of the BVID with a high sensitivity and, moreover, roughly estimate damage location and size. In the near future, by addressing an optimum sensor network form and a proper damage detection algorithm, more effective and robust quantitative impact damage detection system will be developed.

## 5 Conclusions

Impact damage detection system using PPP-BOTDA sensing system is proposed and validated. First, a specific response of the PPP-BOTDA to a non-uniform strain along optical fibers was revealed experimentally and analytically. It was confirmed that non-uniform strain broadens a width of BGS, corresponding to extent of strain gradient. Then the specific response was employed to detect non-uniform strain distribution along the dent of the facesheet induced in damaged area. The proposed system could detect BVID with a high sensitivity and, moreover, roughly estimate damage location and size.

## References

- [1] Zenkert D. (ed.). "The Handbook of Sandwich Construction". EMAS Publishing, 1997.
- [2] Herrmann A. S., Zahlen P. C. and Zuardi I. "Sandwich Structures Technology in Commercial Aviation Present Applications and Future Trends". *Proceedings of the 7th International Conference on Sandwich Structures (ICSS-7)*, Aalborg, Denmark, pp 13-26, 2005.
- [3] Takeda N., Minakuchi S. and Okabe Y. "Smart composite sandwich structures for future aerospace application -damage detection and suppression-: a review", *Journal of Solid Mechanics and Materials Engineering*, Vol. 1, No. 1, pp 3-17, 2007.
- [4] Gates T. S., Su X., Abdi F., Odegard G. M. and Herring H.M. "Facesheet delamination of composite sandwich materials at cryogenic temperatures". *Composites Science and Technology*, Vol. 66, No. 14, pp 2423-2435, 2006.
- [5] Abrate S. "Localized impact on sandwich structures with laminated facings". *Applied Mechanics Reviews*, Vol. 50, No. 2, pp 69-82, 1997.
- [6] Zenkert D., Shipsha A. and Persson K. "Static indentation and unloading response of sandwich beams". *Composites Part B: Engineering*, Vol. 35, No. 6-8, pp 511-522, 2004.
- [7] Edgren F., Asp L. E. and Bull P. H. "Compressive failure of impacted NCF composite sandwich panels - characterisation of the failure process". *Journal of Composite Materials*, Vol. 38, No. 6, pp 495-514, 2004.
- [8] Shipsha A. and Zenkert D. "Compression-after-impact strength of sandwich panels with core crushing damage". *Applied Composite Materials*, Vol. 12, No. 3-4, pp 149-164, 2005.
- [9] Minakuchi S., Okabe Y. and Takeda N. "Segment-wise model" for theoretical simulation of barely visible indentation damage in composite sandwich structures: Part I - Formulation". *Composites Part A: Applied Science and Manufacturing*, Submitted.
- [10] Minakuchi S., Okabe Y. and Takeda N. "Segment-wise model" for theoretical simulation of barely visible indentation damage in composite sandwich structures: Part II - Experimental verification and discussion". *Composites Part A: Applied Science and Manufacturing*, Submitted.
- [11] Bao X., Brown A., Demerchent M. and Smith J. "Characterization of the Brillouin-loss spectrum of single-mode fibers by use of very short (< 10 µs) pulses". *Optical Letters*, Vol. 24, No. 8, pp 501-510, 1999.
- [12] Kishida K., Li C.-H. and Nishiguchi K. "Pulse pre-pump method for cm-order spatial resolution of BOTDA," *Proceeding of the SPIE*, Vol. 5855, pp 559-562, 2005.
- [13] Guzik A., Yamauchi Y., Kishida K. and Li C.-H. "The robust pipe thinning detection method using high precision distributed fiber sensing" *Proceeding of Asia-pacific Workshop on Structural Health Monitoring*, Yokohama, Japan, 24, 2006.
- [14] Minakuchi S., Okabe Y. and Takeda N. "Real-time detection of debonding between honeycomb core and facesheet using a small-diameter FBG sensor embedded in adhesive layer". *Journal of Sandwich Structures and Materials*, Vol. 9, No. 1, pp 9-33, 2007.